

Supporting Information

Cryogenic Infrared Spectroscopy Reveals Remarkably Short NH⁺⋯F Hydrogen Bond in Fluorinated Phenylalanines

Marc Safferthal, Kim Greis, Rayoon Chang, Carla Kirschbaum, Waldemar Hoffmann, Gerard Meijer,
Gert von Helden, and Kevin Pagel*

Table of Contents

Experimental Procedures.....	3
Mass Spectrometry and Infrared Spectroscopy.....	3
Results and Discussion.....	5
Mass Spectra.....	5
Infrared Spectra.....	6
Computational Results.....	8
xyz-Coordinates of Reoptimized Structures.....	10
References.....	10

Experimental Procedures

Mass Spectrometry and Infrared Spectroscopy

Mass and Cryogenic infrared (IR) spectra of the generated ions were recorded using a custom-built instrument that combines mass spectrometry with cryogenic IR spectroscopy in helium droplets as described in the following (Figure S1). The fluorinated phenylalanine derivatives were ionized using a Z-spray nESI source with tip voltages between 0.8–1 kV. The generated ions pass through two ring-electrode ion guides and enter the quadrupole mass filter that allows the selection of analytes by their mass-to-charge ratio. The ions of interest are directed into a hexapole ion trap that is cooled to 90 K by liquid nitrogen. The accumulated ions are thermalized by collisions with helium buffer gas. Superfluid helium droplets are generated by expansion of pressurized helium using a pulsed Even-Lavie valve with a nozzle temperature of 21 K. While traversing the hexapole ion trap, the helium droplets capture ions and cool them to 0.4 K. The doped helium droplets leave the ion trap and enter the detection region where the embedded ions interact with the IR beam generated by the Fritz Haber Institute free-electron laser (FHI FEL)¹. A repeated cascade of photon absorption, excitation of vibrational states, energy redistribution and evaporation of the helium matrix leads to a release of the ions. Hereby, the superfluid helium functions as a cryostat that maintains a constant temperature of 0.4 K. Subsequently, the released ions are detected by a time-of-flight mass analyzer. The IR spectrum is generated by plotting the ion signal over the wavenumber of the laser. The intensities scale non-linearly with the energy of the IR pulse. As a first order correction, the ion count is divided by the photon fluence of the IR macropulse (assuming a constant absorption cross section). Each spectrum is averaged from two scans in the wavenumber region between 1000 and 1800 cm^{-1} .

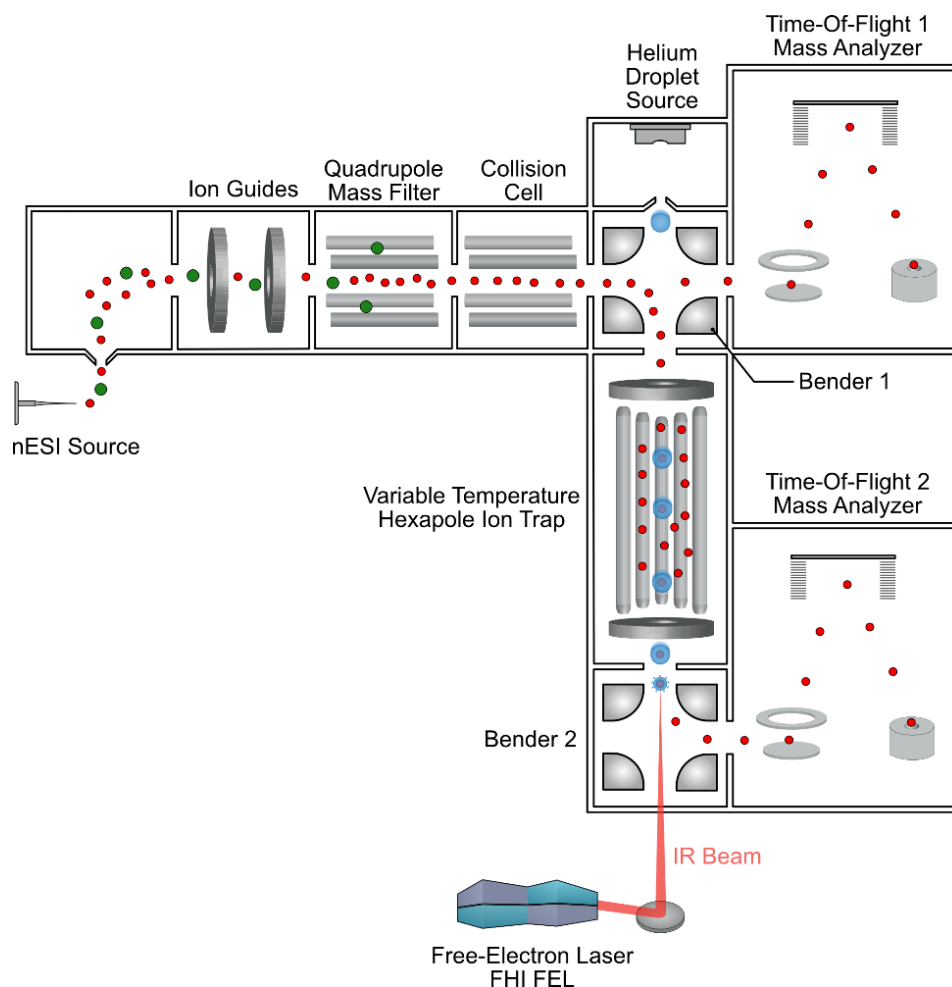


Fig- S1 Schematic representation of the custom-built helium droplet instrument to record mass spectra and cryogenic infrared spectra.

IRMPD spectra of the generated ions were recorded using a previously described custom-built instrument², which combines drift tube ion mobility-mass spectrometry with IRMPD spectroscopy (Figure S2). The fluorinated phenylalanine derivatives were ionized using a nESI source with tip voltages between 0.6–0.8 kV. The generated ions are trapped over several tens of milliseconds and pulsed from a radio frequency (RF) entrance funnel. Subsequently, the ions are pulsed into a linear drift tube (80.55 cm) filled with helium buffer gas (approx. 4 mbar). The analytes are guided through the drift cell by a weak electric field ($10\text{--}15\text{ V cm}^{-1}$), collide with the buffer gas and may be separated by their mass, charge, size and shape. After exiting the ion mobility cell, the ions are radially confined by the exit funnel and guided by ring electrodes into the quadrupole mass filter that allows the selection of analytes by their mass-to-charge ratio. Electrostatic gating with an einzel lens prior to mass-selection allows the selection of ions of a narrow drift time window ($80\text{--}200\text{ }\mu\text{s}$). The m/z - and drift time selected ions are irradiated by an IR beam generated by the FHI FEL¹. Monitoring the photofragmentation by the Wiley-McLaren type time-of-flight mass analyzer as a function of the wavenumber of the tunable laser yields an IR spectrum. Each spectrum is averaged from two scans in the wavenumber region between 1000 and 1800 cm^{-1} .

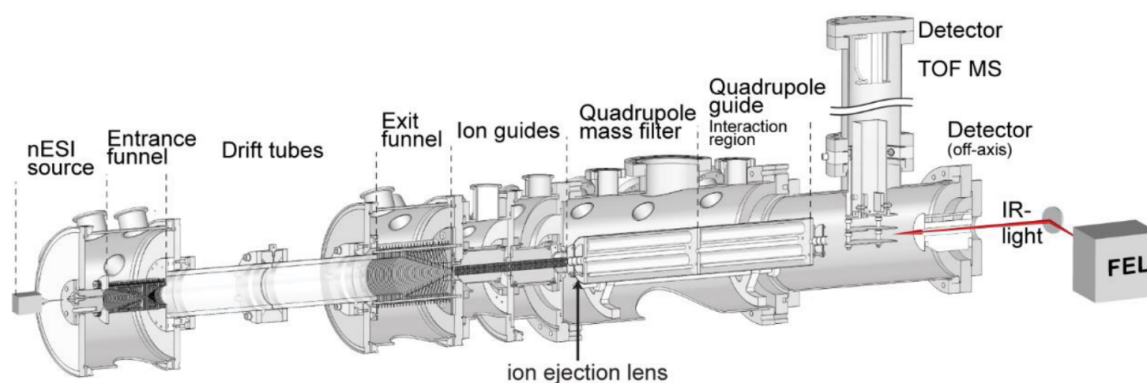


Fig. S2 Schematic representation of the custom-built mass spectrometer that allows to record IRMPD spectra of m/z and drift time-selected analytes.

Results and Discussion

Mass Spectra

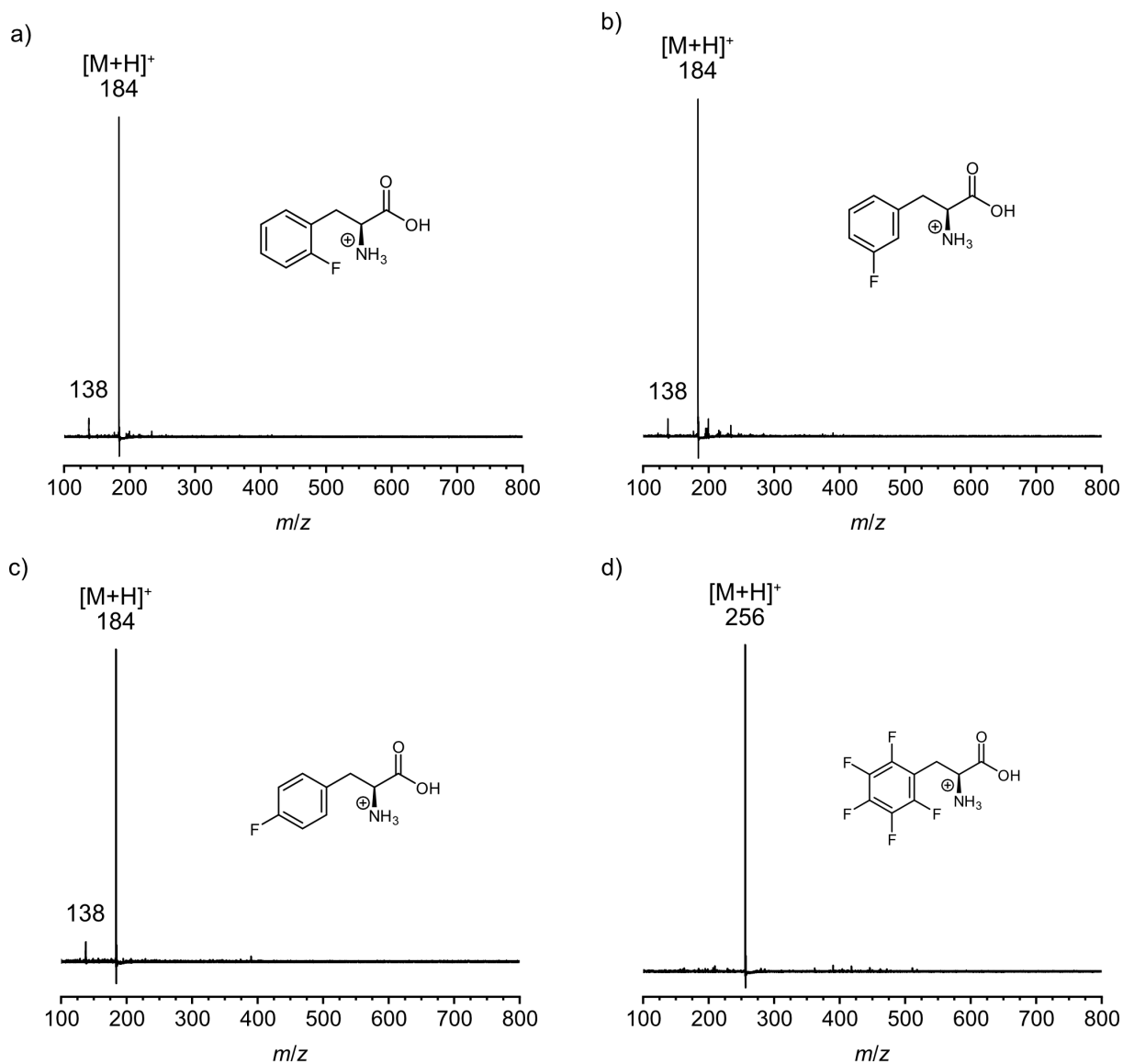


Fig. S3 Mass spectra of a) *ortho*- (***oF*-Phe**) b) *meta*- (***mF*-Phe**) c) *para*- (***pF*-Phe**) and d) pentafluorophenylalanine (***F*₅-Phe**) recorded on the helium droplet instrument. The protonated molecular ions $[M+H]^+$ of the monofluorinated ($m/z = 184$) and pentafluorinated phenylalanines ($m/z = 256$) are generated by nESI. In-source fragmentation of the protonated monofluorophenylalanines generates fragment ions ($m/z = 138$) by a neutral loss of CO and H₂O.

Infrared Spectra

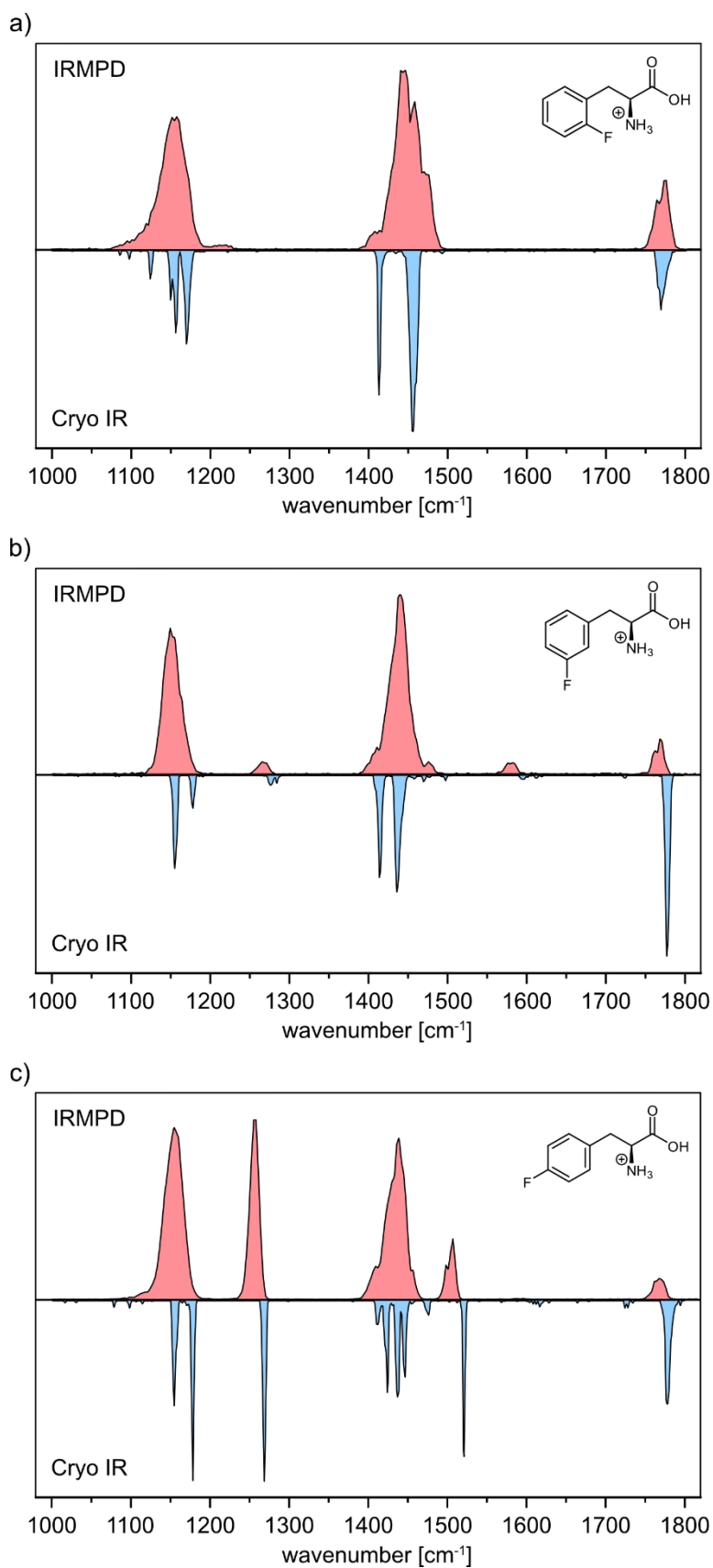


Fig. S4 Comparison of experimental IRMPD and Cryogenic IR spectra of the a) *ortho*- (***oF-Phe***) b) *meta*- (***mF-Phe***) and c) *para*-fluorophenylalanine (***pF-Phe***) cations.

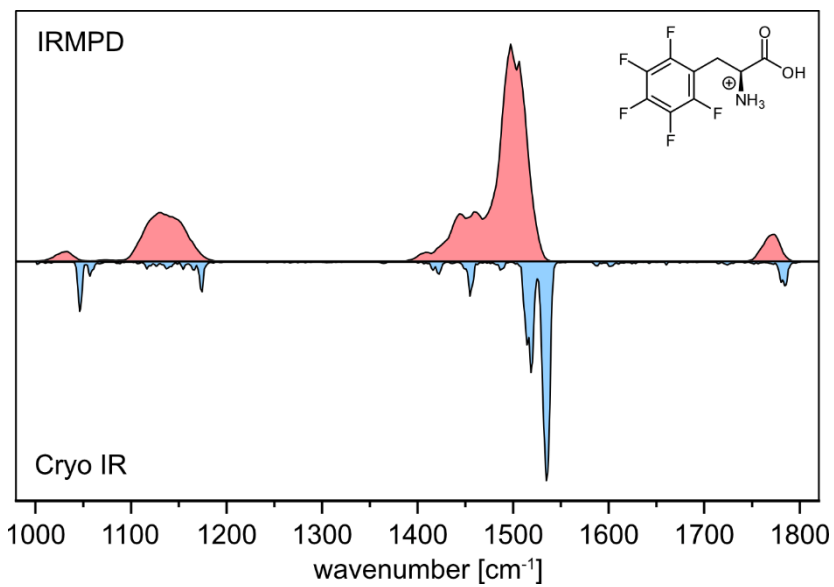


Fig. S5 Comparison of experimental IRMPD and Cryogenic IR spectra of the pentafluorophenylalanine (F₅-Phe) cations.

Computational Results

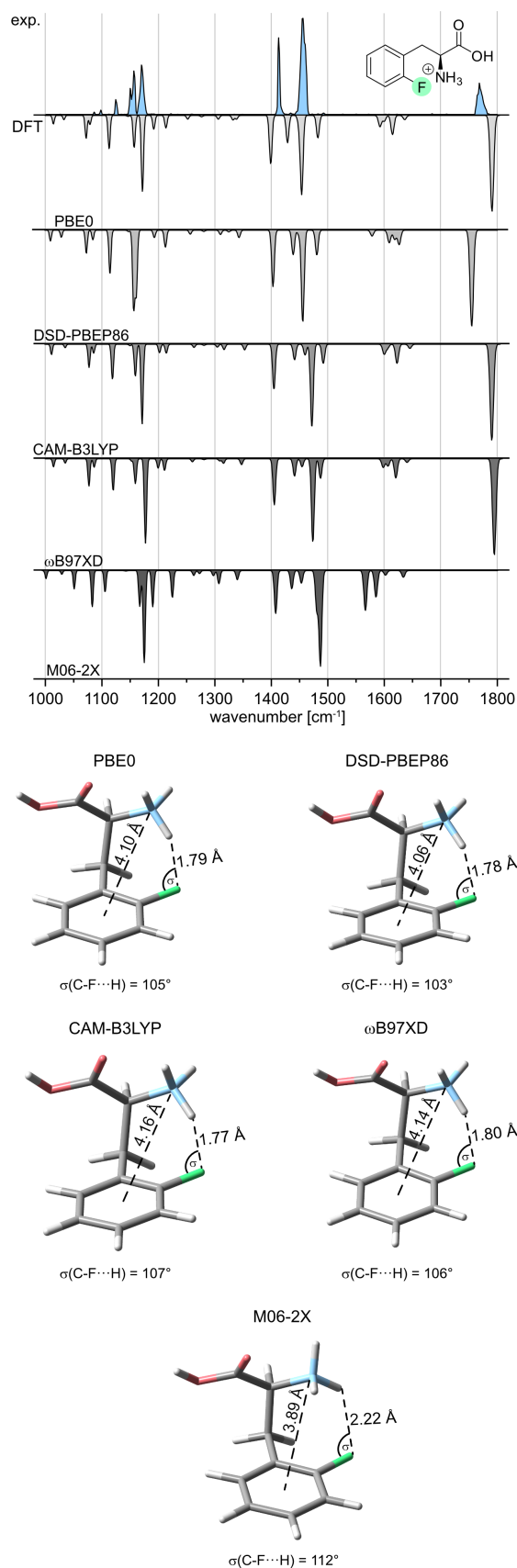


Fig. S6 Comparison of frequencies and structures of **oF-Phe** conformer A at different levels of theory. Experimental IR spectra are depicted as light blue traces. Computed spectra of conformer A are shown as gray inverted traces. The structures are depicted below the IR spectra with relevant geometrical parameters.

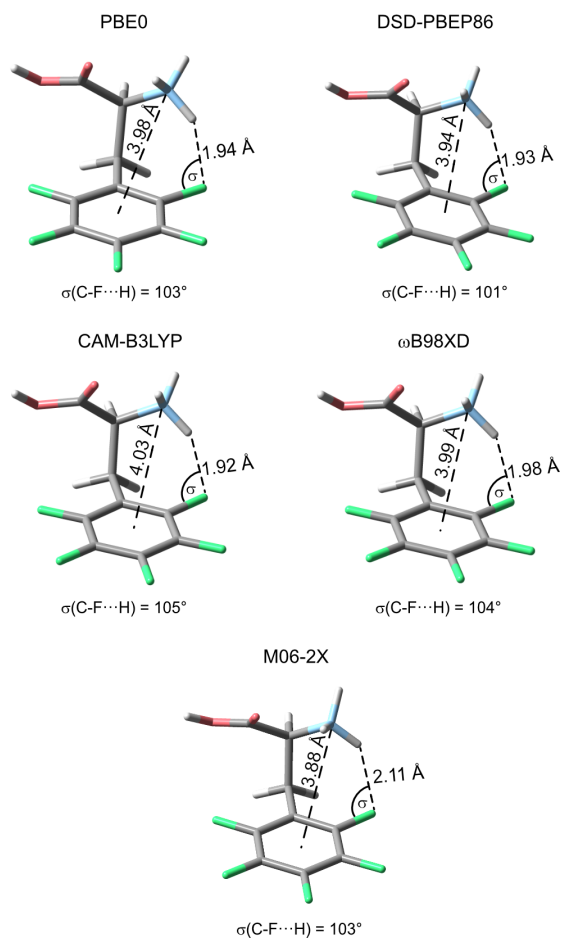
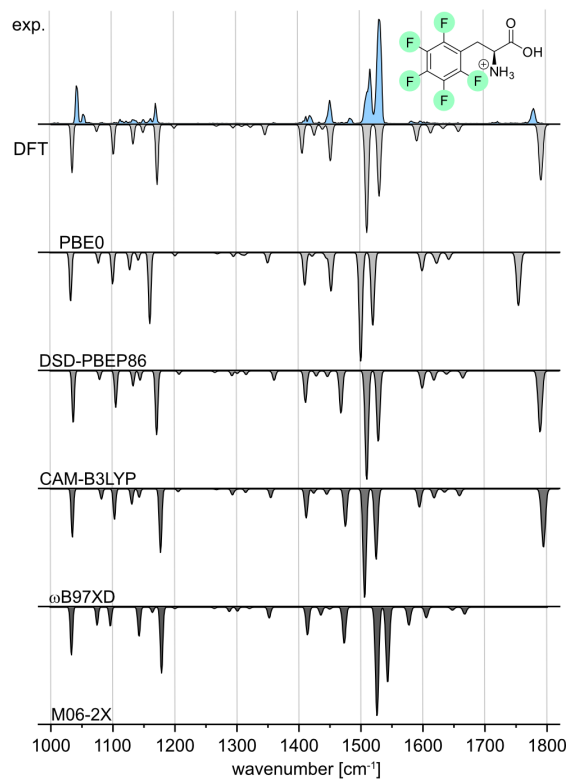


Fig. S7 Comparison of frequencies and structures of $\text{F}_5\text{-Phe}$ conformer A at different levels of theory. Experimental IR spectra are depicted as light blue traces. Computed spectra of conformer A are shown as gray inverted traces. The structures are depicted below the IR spectra with relevant geometrical parameters.

Table S1 GA parameters used in initial search. A detailed description of the parameters can be found in the original paper of FAFOOM³.

	Parameter	Value
Molecule	Distance_cutoff_1	1.2
	Distance_cutoff_2	2.15
	Rmsd_cutoff_uniq	0.25
GA settings	Popsize	10
	Prob_for_crossing	0.95
	Prob_for_mut_torsion	0.8
	Fitness_sum_limit	1.2
	Selection	Roulette wheel
	Max_mutations_torsion	3

xyz-Coordinates of Reoptimized Structures

xyz-Coordinates of all reoptimized geometries at the PBE0+D3/6-311+G(d,p) level of theory can be found in a separate document "coordinates.xyz".

References

1. W. Schöllkopf, S. Gewinner, H. Junkes, A. Paarmann, G. von Helden, H. Bluem and A. M. M. Todd, *Proc. SPIE-Int. Soc. Opt. Eng.*, 2015, **9512**, 95121 L.
2. S. Warnke, J. Seo, J. Boschmans, F. Sobott, J. H. Scrivens, C. Bleiholder, M. T. Bowers, S. Gewinner, W. Schöllkopf, K. Pagel and G. von Helden, *J. Am. Chem. Soc.*, 2015, **137**, 4236-4242.
3. A. Supady, V. Blum and C. Baldauf, *J. Chem. Inf. Model.*, 2015, **55**, 2338-2348.